Interplanetary Coronal Mass Ejections in the Near-Earth Solar Wind During 1996-2002

H. V. Cane[1] and I. G. Richardson[2]
NASA Goddard Space Flight Center, Greenbelt, Maryland

Abstract.
We summarize the occurrence of interplanetary coronal mass ejections (ICMEs) in the near-Earth solar wind during 1996-2002, corresponding to the increasing and maximum phases of solar cycle 23. In particular, we give a detailed list of such events. This list, based on in-situ observations, is not confined to sub-sets of ICMEs, such as "magnetic clouds" or those preceded by 'halo' CMEs observed by the SOHO/LASCO coronagraph, and provides an overview of 214 ICMEs in the near-Earth solar wind during this period. The ICME rate increases by about an order of magnitude from solar minimum to solar maximum (when the rate is ~ 3 ICMEs/solar rotation period). The rate also shows a temporary reduction during 1999, and another brief, deeper reduction in late 2000–early 2001, which only approximately track variations in the solar 10 cm flux. In addition, there are occasional periods of several rotations duration when the ICME rate is enhanced in association with high solar activity levels. We find an indication of a periodic variation in the ICME rate, with a prominent period of ~ 165 days similar to that previously reported in various solar phenomena. It is found that the fraction of ICMEs that are magnetic clouds has a solar cycle variation, the fraction being larger near solar minimum. For the subset of events that we could associate with a CME at the Sun, the transit speeds from the Sun to the Earth were highest after solar maximum.

1. Introduction

Material in the solar wind now believed to be the interplanetary counterparts of coronal mass ejections (CMEs) at the Sun has been identified since the early years of solar wind observations. By the early 1980s, most of the characteristic signatures of such material, which we here term "interplanetary coronal mass ejections" (ICMEs) had been identified, as reviewed by *Gosling* [1990] and *Neugebauer and Goldstein* [1997]. (Older terms used for ICMEs include "driver gas" and "ejecta"). Combined in-situ measurements by the Helios spacecraft off the limbs of the Sun and observations by the Solwind coronagraph demonstrated the clear association between CMEs at the Sun and shocks and ICMEs subsequently detected in the interplanetary medium [*Sheeley et al.*, 1985]. Solar wind plasma signatures of ICMEs include abnormally low proton temperatures [e.g., *Gosling et al.*, 1973; *Richardson and Cane*, 1995], low electron temperatures [e.g., *Montgomery et al.*, 1974], and bi-directional suprathermal electron strahls [e.g., *Zwickl et al.*, 1983; *Gosling et al.*, 1987]. Plasma compositional anomalies have also been identified in ICMEs including enhanced plasma helium abundances relative to protons [e.g., *Hirshberg et al.*, 1972; *Borrini et al.*, 1982] and occasional enhancements in minor ions (in particular iron) [*Bame et al.*, 1979; *Mitchell et al.*, 1983; *Ipavich et al.*, 1986]. Enhanced Fe charge states have also been reported [*Bame et al.*, 1979; *Fenimore*, 1980; *Ipavich et al.* 1986; *Lepri et al.*, 2001]. Such enrichments suggest that the plasma inside ICMEs originates in the low corona. Energetic particle signatures include bi-directional energetic protons [e.g., *Palmer et al.*, 1978; *Marsden et al.*, 1987; *Richardson and Reames*, 1993] and cosmic rays [*Richardson et al.*, 2000], energetic particle intensity depressions (Forbush Decreases) [e.g., *Morrison*, 1956; *Barnden*, 1972; *Cane et al.*, 1994] and unusual solar energetic particle (SEP) flow directions [*Richardson et al.*, 1991; *Richardson and Cane*, 1996]. The bi-directional particle flows (suprathermal electron strahls and energetic particles), unusual solar particle event flows, and energetic particle intensity depressions are consistent with the presence within many ICMEs of regions of looped magnetic field lines rooted at the Sun at both ends.

A subset of ICMEs have simple flux-rope like magnetic fields characterized by enhanced magnetic fields that rotate slowly through a large angle. Such "magnetic clouds" [*Burlaga et al.*, 1981; *Klein and Burlaga*, 1982] have received considerable attention because the magnetic field configuration is amenable to simple modeling [e.g., *Lepping et al.*, 1990; *Osherovich and Burlaga*, 1997, and references therein], and may be consistent with helical structures occasionally present in coronagraph observations of CMEs [e.g., *Dere et al.*, 1999]. Magnetic clouds are also responsible for some major geomagnetic storms [e.g., *Webb et al.*, 2000].

As has been noted by many authors however, [e.g., *Zwickl et al.*, 1983; *Crooker et al.* 1990; *Richardson and Cane*, 1993, 1995; *Neugebauer and Goldstein*, 1997], individual signatures may not be detected in all ICMEs, either because

[1]Also at School of Mathematics and Physics, University of Tasmania, Hobart, Australia.

[2]Also at Department of Astronomy, University of Maryland, College Park.

Paper number .
0148-0227/03/$9.00

they are not present, or as a result of instrumental limitations or data gaps. Some signatures have been reported relatively infrequently. For example, *Zwickl et al.* [1982] found only three distinct He^+ events in 8 years of IMP 7 and 8 and ISEE 1 and 3 observations. Others, such as proton temperature depressions, are generally present [e.g., *Richardson and Cane*, 1995]. Furthermore, even if several signatures are present in an ICME, they do not necessarily coincide exactly. Hence, to make a comprehensive identification of ICMEs, observations of as many signatures as possible should be considered. Those signatures that are most frequently present are of particular value.

Our own interest in ICMEs lies in several areas. One is their effects on energetic particles. Our studies suggest that these effects generally do not depend strongly on the nature of the in-situ signatures. This is not too surprising since presumably it is the large scale topology of the ICME field lines (i.e., whether they are predominantly closed) that is important in modulating the particle intensity, not the magnetic fields that are observed along the particular trajectory of a spacecraft through the ICME. Another of our interests is the contribution of ICMEs to geomagnetic activity, both storms and long-term averages [e.g., *Cane et al.*, 2000; *Richardson et al.*, 2001a, 2002]. Hence, as a contribution to such studies, we have maintained a list of ICMEs at Earth which extends back to the earliest in-situ observations. This is relatively comprehensive because our interest is not limited to a sub-set of events with particular signatures. This list has evolved and expanded with our various studies related to ICMEs in the inner heliosphere, many of which are referenced in this paper. These studies also illustrate many examples of ICMEs which help to demonstrate the wide event-to-event diversity in the various ICME signatures and their inter-relationships.

In this paper, we concentrate on events in 1996-2002, during the increasing phase and maximum of solar cycle 23. During the current solar cycle, coronal mass ejections at the Sun have been regularly monitored by the SOHO spacecraft since its launch in December 1995. The Large Angle Spectrometric Coronagraph (LASCO) [*Brueckner et al.* 1995] is more sensitive to structures moving out of the plane of the sky than previous coronagraphs and has observed a significant number of CMEs which surround the Sun (angular extents of 360°) that may be directed approximately along the Sun-Earth line (similar events originating on the backside of the Sun and moving away from Earth are also seen). Various studies have linked apparently Earthward-directed CMEs with in-situ observations of ICMEs at 1 AU, focusing, for example, on their geomagnetic effects or transit times [e.g., *Webb et al.*, 2000; *Cane et al.*, 1998a, 2000; *Gopalswamy et al.*, 2000, 2001; *Wang et al.*, 2002]. However, such studies have not attempted to provide a comprehensive survey of ICMEs in the vicinity of Earth, starting from the in-situ observations, which is the purpose of the present paper.

2. The List

The principle data sets we routinely use for the identification of potential ICMEs are solar wind plasma and magnetic field observations. A major reason is that such data are readily available since the beginning of the space era. Since it appears to be a common feature of most ICMEs [e.g., *Richardson and Cane*, 1993, 1995], one of our primary identifying signatures is the occurrence of abnormally low proton temperatures. To identify such plasma, we use the method of *Richardson and Cane* [1993, 1995] which compares, point by point, the observed proton temperature (T_p) with the "expected" temperature (T_{ex}) appropriate for "normally-expanding" solar wind with the observed solar wind speed (V_{sw}). The expected temperature is essentially the typical temperature found in normal solar wind with speed V_{sw}, and is inferred using the well-established correlation between the solar wind speed and T_p [e.g., *Burlaga and Ogilvie*, 1973; *Lopez*, 1987] which however may be slightly instrument-dependent (see the discussion in *Neugebauer et al.* [2002]). We find that many ICMEs are characterized by $T_p/T_{ex} < 0.5$ [e.g., *Richardson and Cane*, 1995].

Having identified periods of interest based on T_p, we typically examine magnetic field observations during these periods, ideally at a time resolution of 5 minutes or less. Frequently in ICMEs, the field is directed far from the Parker spiral in azimuth, or has large out-of-the-ecliptic components. A useful characteristic is a reduction in the level of field fluctuations which can be identified by eye in data with this time resolution. In some cases, a clear magnetic cloud signature is present. In other ICMEs, there is often evidence of an organized field rotation, but the signature does not conform to the strict cloud definition of *Burlaga et al.* [1981] and *Klein and Burlaga* [1982]. Alternatively, there may be no distinct rotation, two extremes being a magnetic field that is relatively constant in direction and one that includes many discontinuities in direction which may be related to internal structure. In summary, most often, a likely ICME interval can be inferred from reduced fluctuations and some degree of organization in the magnetic field, and is bounded by distinct magnetic field discontinuities which may be accompanied by abrupt changes in plasma parameters. Typically, this interval corresponds reasonably well with the T_p depression, though in some ICMEs they may differ significantly. There are also occasional ICMEs (based on other the presence of other ICME signatures) that do not have well characterized field signatures. One other point to note is that although ICMEs can include strong magnetic fields, such fields are not characteristic of all ICMEs.

We also consider additional complementary signatures that may be indicative of the presence of ICMEs. One is the occurrence of interplanetary shocks. Fast ICMEs may generate shocks ahead of them, so that an ICME is often located a few hours following passage of a shock. Note however, that an ICME is not present following every shock because the flanks of a shock extend well beyond the associated ICME [e.g., *Borrini et al.*, 1982; *Cane*, 1988; *Richardson and Cane*, 1993]. If the ICME is not sufficiently fast to generate a shock, there is sometimes evidence of an upstream wave-like disturbance that has not steepened into a shock. In other cases, if the ICME is convected out with the ambient solar wind, there may be no clear upstream feature. In addition to examining the solar wind data for evidence of shocks, and referring to available lists of shocks, we refer to reports of geomagnetic storm sudden commencements (SCs), which are generally (but not always) associated with shocks passing the Earth (although almost all stronger shocks are accompanied by SCs the exceptions being when the geomagnetic field is already disturbed). Such reports are particularly helpful when no in-situ solar wind observations are available, though this is not a concern during the period considered in this paper.

We routinely compare the solar wind observations with simultaneous energetic ($\sim$ 1 – 220 MeV) particle observations from the Goddard Medium Energy (GME) experiment on IMP 8 [*McGuire et al.*, 1986] and higher energy (GeV) cosmic ray observations from neutron monitors. Solar energetic particle (SEP) events can help to relate shocks and ICMEs with specific solar events occuring $\sim$ 2 days earlier via their intensity-time profiles. An abrupt SEP intensity decrease a few hours following a shock usually indicates entry into the ICME, because the shock-accelerated ions have difficulty entering the closed field lines of the ICME. An abrupt decrease in the galactic cosmic ray intensity may also occur at this time. When combined with the preceding decrease that often occurs at shock passage, this produces the classic "two-step" cosmic ray Forbush decrease [*Cane*, 2000, and references therein]. The IMP 8 GME anti-coincidence guard is a useful cosmic ray monitor for this purpose, provided that the background from solar particle events is not too high [e.g., *Cane et al.*, 1994, 1998a]. The rigidity response is also lower than that of neutron monitors which means that a larger counting rate depression will be seen in response to an ICME since the depression size decreases with increasing rigidity. In general, arrival of an ICME at Earth produces some detectable decrease in the cosmic ray intensity measured by IMP 8, followed by a recovery after the ICME has passed by. With familiarity with the data, ICME-related depressions can frequently be identified even without first referring to the solar wind parameters. However, the particle signatures can also be more subtle, and merely add to the evidence of the presence of an ICME. Although energetic particle observations play a supporting role to plasma and magnetic field observations when such observations are continuously available (as in cycle 23), they are useful in assessing the presence of solar wind structures when solar wind data are intermittent or non-existent such as in the early space era and in cycle 22 [e.g., *Cane et al.*, 1996]. The IMP 8 GME also provides information on the presence of bi-directional energetic particle flows, which can be indicative of ICMEs, provided that the particle intensity is sufficiently high and the spacecraft is located in the solar wind [e.g., *Richardson et al.*, 2001b, and references therein].

One of the most widely used signatures in ICME identification is the presence of bi-directional solar wind electron strahls (BDEs). Although many researchers regard this as the most reliable signature, and indeed some studies identify ICMEs largely on this signature, we do not use BDEs as the primary signature. One reason, more relevant for our longer-term studies, is that BDE observations are only available for relatively limited intervals since in-situ solar wind observations began. Another reason is that BDEs are known to be absent in some regions of ICMEs, apparently where ICME magnetic field lines have reconnected with the ambient solar wind, removing the heat flux in one direction [*Gosling et al.*, 1995]. In some of our previous studies, we noted that occasionally, BDEs are detected that do not appear to be associated with ICMEs, or may extend beyond ICME regions that are distinguished in other data [e.g., *Richardson and Cane*, 1993]. Observations from the ACE spacecraft *Gosling et al.* [2001] also suggest that electron distributions may be complicated by counterstreaming set up by mirroring at magnetic field enhancements. It would have been interesting to compare our ICME identifications with intervals of BDEs but unfortunately there is no list of BDEs in the public domain for most of the period of our study at the time of writing.

In our ICME identification, we do not currently routinely incorporate plasma composition data. Again, one reason is that such data have been less consistently available in the past than the basic solar wind parameters. In addition, anomalous solar wind charge states and compositions are a subject of ongoing research and their association with ICMEs remains to be fully explored. Thus, our independent ICME list can provide a useful cross-reference for such studies [e.g., *Lepri et al.*, 2001].

The estimated event boundaries given in this paper are therefore inferred from a consensus of the available signatures with an emphasis on those in the solar wind plasma and magnetic field. Typically these boundaries can be associated with distinct plasma/magnetic field discontinuities. In other cases, the boundaries are less pronounced, but can be identified to within a relatively short period.

The probable ICMEs that we have identified are listed in Table 1. The first column indicates the estimated time of the related disturbance in the upstream solar wind, if present. This may be a distinct shock, or a small increase in the solar wind parameters which suggests a "bow-wave". The SC time is given if one occurred. In this case, the SC strength (fifth column) has been calculated by the method of *Cane* [1985] in which the SC strengths reported by stations at geomagnetic latitudes of $5 - 50^{o}$ are averaged. *Cane* [1985, 1988] showed that this parameter is correlated with the shock compression ratio. Values of 0 and ... indicate that either a very weak or no SC was reported, respectively. This parameter is also used to validate associations. In some cases when an SC did not occur the disturbance time is the time of shock passage at the ACE spacecraft, denoted by (A) (ACE shocks confirmed from the website http://www.bartol.udel.edu/ ~chuck/ace/ACElists/obs_list.html). The second and third columns give the estimated start and end times of the ICME, while the following column indicates the quality of the estimated boundary times (1 = most accurate; 3 = ill-defined; note that this parameter does not necessarily reflect the confidence of the ICME identification). The sixth and seventh columns give the mean speed of the ICME and the maximum speed in the post-disturbance region, which may occur either in the "sheath" ahead of the ICME or in the ICME itself. The next column gives the mean field strength in the ICME. In the following column, "2" indicates whether the ICME has been reported as a magnetic cloud which can be modeled by a force-free flux-rope (at http://lepmfi.gsfc.nasa.gov/mfi/mag_cloud_pub1.html; for recent events since May 2002, not covered by this magnetic cloud list, we have assessed whether the ICME is likely to meet the criteria for a magnetic cloud). If a more subjective assessment suggests evidence of a relatively organized field rotation within the ICME, but a magnetic cloud has not been reported, a "1" is indicated. A "0" indicates that the field shows little evidence of rotation. The third last column gives the minimum value of the geomagnetic *Dst* index (stronger activity is denoted by an increasingly negative value). The disturbance transit speed to 1 AU is indicated in the next column for those events where the associated CME observed by LASCO can be identified. The time of first observation of this CME in the LASCO C2 coronagraph is indicated in the last column. An "H" following the date indicates that the coronagraph signature encircled the Sun (i.e., had an angular extent of 360^{o}, commonly called a 'full halo' event). When making these associations, we have only

considered CMEs with angular extents of at least 100°. For almost all of the energetic events, the CME association is easily made because the shock driven by a fast ICME continuously accelerates energetic particles which directly link the passage of the shock at the Earth to the time of a specific CME at the Sun. For a variety of reasons, no CME is indicated for many of the ICMEs. One reason is that there are no LASCO observations around the time when the associated CME might have occurred, indicated by "dg" (data gap). In addition to the extended suspension of SOHO operations in June-October 1998, there are shorter interruptions to LASCO observations, often of several days duration, that are noted in the preliminary lists of LASCO CMEs. Where there is a LASCO data gap but the associated solar event is clearly identifiable from other data, the time is indicated in brackets. There are other cases where LASCO observations are available but show no evidence of a large CME during the several days prior to arrival of the ICME at Earth, such as for the June 19, 1997 event discussed by *Richardson et al.* [1999]. It is likely that such ICMEs are associated with Earthward-directed CMEs that are not sufficiently dense to be detectable by LASCO. In other cases, one or more wide CMEs may be reported in this time range, but examination of the related solar activity as observed for example by EIT suggests that these CMEs originated near the solar limbs or from the backside of the Sun and were unlikely to give rise to ICMEs at Earth based on the conclusions of our previous studies [e.g., *Richardson and Cane,* 1993; *Cane and Richardson,* 1995; *Cane et al.,* 1997, 2000]. At times of high activity, there may be several wide CMEs with reasonable locations reported prior to an ICME so that it is difficult to relate the ICME to a specific CME. In these, and other doubtful cases, the time of the most likely associated CME is noted and followed by a '?'. The CME properties we have used here are from the S. Yashiro and G. Michalek catalog available from the World Wide Web at http://cdaw.gsfc.nasa.gov/CME_list/. We have also referred back to the original LASCO observer reports since these are of value in indicating the general location of the related solar activity or whether the event was likely to be back-sided and therefore of little interest for relating with in-situ observations at Earth. Although we have focused on wide CMEs, we recognize of course that there are many more narrower CMEs observed by LASCO. However, our expectation is that these CMEs are unlikely to be related to ICMEs at Earth. Another point to note is that although we have attempted to isolate individual ICMEs, it is possible that some events are conglomerations of ICMEs from multiple solar injections or, conversely, a series of events may be multiple encounters with a single ICME. However, we doubt that either of these situations occurs very often because, as discussed below, the relative change in ICME rate from solar minimum to maximum is similar to that in the CME rate. In Table 1 we indicate by 'e' in the final column a small number of ICME periods that probably resulted from multiple CMEs (cf. *Burlaga et al.* [2002]).

In making the CME–ICME associations, we have found a good correlation between the maximum solar wind speed observed in situ at 1 AU in the sheath or ICME (V_{max}) and the transit speed (V_T) of the disturbance driven by the ICME to 1 AU for those events with a confident association (Figure 1). (A similar result has been previously obtained by *Cliver et al.* [1990].) In cases where the CME-ICME association is more uncertain, this relationship can be used to indicate whether a particular association is at least plausible. For example, Figure 1 suggests that an ICME associated with V_{max} = 500 km/s is unlikely to be associated with a solar event < 42 hours earlier that would require a transit speed above ~ 1000 km/s. Note that the transit speed is generally higher than V_{max} (the dashed line indicates $V_T = V_{max}$), implying that the disturbances decelerate en route to 1 AU. Furthermore, this deceleration is greater for higher transit speeds, consistent with the results of previous studies [e.g., *Woo et al.* 1985]. For lower speed events, the transit and in-situ speeds are more comparable and similar to typical solar wind speeds (~ 400 km/s), consistent with their convection with the solar wind. Although it is possible to infer ICME acceleration rates and initial speeds as a function of V_{max} or transit speed from the results in Figure 1 by making a simple assumption such as a constant acceleration/deceleration rate in the solar wind [e.g., *Gopalswamy et al.*, 2001], since such an assumption is questionable, we have not pursued this further.

3. Occurrence Rates

As might be expected, the yearly number of ICMEs increases with solar activity levels. During solar minimum conditions in 1996, only four ICMEs were identified, compared with 53 in 2000 and 47 in 2001 (see Table 2). Thus, the ICME rate increased by about an order of magnitude from ~one every 3 months at solar minimum to ~one per week at solar maximum. These are average rates. At times of exceptionally high activity such as in May 1998, July 2000 or April 2001, the rate increases to several ICMEs/week (e.g., 5 ICMEs were observed between July 11-18, 2000). *Burlaga et al.* [1984] and *Cliver et al.* [1987] have discussed the consequences of such systems of transient flows passing the Earth during previous solar cycles. The decrease in the ICME rate in 1999 was noted in our previous study that only extended to this time [*Cane et al.*, 2000]. The rate increased again in the subsequent two years. A decline in the fraction of CME-related solar wind at Earth in 1999 is also evident in Figure 3 of *Richardson et al.,* [2002], together with a compensating increase in the contribution from corotating high-speed streams originating in low-latitude coronal holes, which were particularly prominent in 1999 [e.g., *Luhmann et al.,* 2002]. Thus, the temporary decline in the ICME rate at Earth is associated with a restructuring of the near-ecliptic solar wind.

Figure 2a shows the variation in the ICME rate during 1996-2002 in greater detail, specifically the number of ICMEs at Earth/Carrington rotation (CR) expressed as a 3-rotation running mean. The main increase in the ICME rate, to ~ 2 – 3/CR, commenced early in 1997 and extended through this year. Overall, the rate has not varied greatly from this value during solar maximum, with the exception of short intervals, typically of ~ 3 rotation duration, when the ICME rate was enhanced due to major solar activity, as mentioned above. In addition, there is a decrease in the ICME rate to ~ 1 – 2/CR during much of 1999 and a short duration decrease in late 2000-early 2001. A typical rate of ~ 3 ICMEs/CR around solar maximum represents ~ 3% of the LASCO CME rate near maximum of ~ 4/day (O. C. St Cyr, private communication, 2002). It is also an order of magnitude higher than the ICME rate during 1996 at solar minimum (~ 0.3 ICMEs/CR), which is ~ 2% of the LASCO CME rate during this year (0.63/day [*St. Cyr et al.*, 2000]).

To compare the variations in the ICME rate with a measure of solar activity levels, Figure 2b shows the solar 10 cm flux recorded by the Dominion Radio Astrophysical Observatory. Note the two maxima, during the first half of 2000 and second half of 2001. (The smoothed sunspot number also shows two maxima but the peak in April 2000 was slightly higher relative to the peak in November 2001 than in the 10 cm flux.) Assuming that our ICME rate is proportional to the CME rate, it can be seen that the rate does not follow the solar activity quite as closely as suggested by the work of *Webb and Howard* [1994]. The most significant difference is the reduction in 1999 which is not matched by a similar decrease in the 10 cm flux. The observations for 2002 show evidence for the expected reduction in the ICME rate as the solar cycle declines, the 3-rotation mean rate never exceeding 3 ICMEs/CR.

An interesting feature of Figure 2a is the suggestion of periodicity in the intervals of enhanced ICME rate. A Lomb frequency analysis of the (unsmoothed) CME rate for 1996-November 2002 indicates a dominant, statistically significant component with a period of 164.7 days. This period is particularly interesting since it is close to the "154-day" periodicity identified in various solar phenomena during previous solar cycles (see *Cane et al.* [1998b] and references therein). The apparent periodicity in the ICME rate suggests that the fundamental periodicity at the Sun identified in previous solar cycles is present in the current cycle, as also noted in energetic particle intensities at 1 and 5 AU in 1998-99 by *Dalla et al.* [2001].

4. Average Properties of ICMES

Table 2 lists the average properties of ICMEs and their variation as a function of year. Another clear solar cycle variation is evident in the fraction of the ICMEs that are magnetic clouds. This decreased from 100% (though with poor statistics) in 1996, to $\sim$ 16% in 2000-2001, and appears to be recovering in 2002 as activity declines. Data from previous solar cycles support such a solar cycle variation (I. G. Richardson and H. V. Cane, The fraction of interplanetary coronal mass ejections that are magnetic clouds, manuscript in preparation). Average speeds of individual ICMEs varied from 270 to 850 km/s with a mean value of 454±6 km/s. The mean speed shows a $\sim$ 100 km/s increase from solar minimum to maximum. This increase is also evident in Figure 4b of *Richardson et al.* [2002] which, however, suggests that this trend may be specific to cycle 23 since the previous two solar cycles show instead a temporary minimum in mean ICME speeds near solar maximum. The transit speed of the associated disturbance is also ordered by the phase of the solar cycle in that there were only 3 shocks with transit speeds above 1000 km/s during the $\sim$ 4.5 years before solar (smoothed sunspot) maximum (April 2000) versus 11 thus far in the first $\sim$ 2.5 years after maximum (Figure 3). It is such fast shocks that are responsible for large >10 MeV particle events [*Cane et al.*, 1988].

Average magnetic field strengths in individual ICMEs varied from 3 to 39 nT with a mean value of 9.9±0.3 nT. There is a slight decrease in average fields from minimum to maximum. This is primarily related to the fact that the fraction of magnetic clouds decreased towards maximum. The average ICME size in the radial direction (the product of the duration and average speed) was 0.33±0.01 AU. For those events (typically the more energetic) that we could associate with a solar event (usually an Hα flare), the longitudes were predominantly within ±50° of central meridian, as shown by the 'source' longitude distribution in Figure 4. This result suggests that ICMEs associated with the more energetic solar events have angular extents of up to $\sim$ 100°, as previously inferred by *Richardson and Cane* [1993]. An interesting feature of the distribution is the occasional presence at Earth of ICMEs from far western regions but not from far eastern regions. A similar asymmetry in the source longitude distribution was found by *Cane* [1988] for bidirectional suprathermal electron strahls (which, as noted above, may be indicative of ICMEs) in cycle 21, suggesting that this is a general feature. A possible explanation for the asymmetry in Figure 4 (see also Figure 3a of *Wang et al.* [2002]) is that some CMEs preferentially occur to the east of the active region where the associated flare occurred (i.e., the flare is not necessarily centered beneath the CME). This has a natural explanation in terms of differential rotation, which causes shearing and eastward motion of erupted magnetic flux in both hemispheres of the Sun.

5. Solar-terrestrial relations

There has been much emphasis in recent years on the relationship between CMEs of large angular extent observed by LASCO that appear to be moving towards or away from the Earth approximately along the Sun-Earth line (i.e., halo CMEs) and the effects of the associated ICMEs when they arrive at Earth about two days later [e.g., *St. Cyr et al.*, 2000; *Webb et al.*, 2000]. However, as we have noted previously [*Cane et al.*, 2000], there is certainly not a simple one-to-one relationship between large CMEs (with associated frontside solar activity) and ICMEs observed subsequently at Earth. We concluded that in 1996-1999, about a third of the ICMEs detected at Earth were not preceded by a >140° CME evident in LASCO observations. In Table 1 it is evident that we cannot associate many of the ICMEs with large CMEs. In some cases this is because there were no LASCO observations around the probable time that the related CME might have occurred (indicated by "dg"). We conclude that a significant fraction, about a half, of the ICMEs detected at Earth do not have a probable association with a large CME observed by LASCO. *Cane et al.* [2000] also found that only about half of the frontside >140° width CMEs observed by LASCO subsequently encountered the Earth. For the additional years of the current study (2000 and 2001), we find that even if only those events which surround the Sun are considered (i.e., full halo events with angular extents of 360°), the fraction is only about 39%. This contrasts with the situation in 1997 when all the frontside full halo CMEs resulted in the detection of ICMEs near Earth (see also *Zhao and Webb* [2002]). We suggest that when the corona is close to its solar minimum configuration, 360° coronagraph events result from CMEs directed at (or away from) the Earth as is commonly assumed. However later in the solar cycle (approaching and during solar maximum), the corona is much more complex and coronagraph observations may include more contributions from other phenomena such as streamer deflections [e.g., *Sheeley et al.*, 2000] that give rise to features surrounding the Sun even when the associated CME is not directed at the Earth.

In Figure 5 we compare the disturbance transit speeds to 1 AU with the speeds of the associated CMEs. Although the CME speeds are projected against the plane of the sky

and do not represent the true Earthward-directed speeds of the CMEs, there is nonetheless some degree of correlation as we have noted previously [*Cane et al.*, 2000]. The upper envelope of the distribution is given approximately by $V_{tr} = 400 + 0.8V_{CME}$ (this defines the minimum transit time for a given CME speed) while the lower envelope is approximately $V_{tr} = 0.37V_{CME}$. The observed transit speeds do not fall below $\sim$ 400 km/s. Given the considerable scatter among the data points however, it seems unrealistic to expect that the transit speed for a given CME speed can be predicted precisely. Note that we consider here the *disturbance* speed because this corresponds to the earliest time when a CME may produce a disturbance at Earth. *Gopalswamy et al.* [2000, 2001] have developed an empirical model to predict *ICME* arrival times based on LASCO CME speeds. For CME speeds below $\sim$ 700 km/s, an ICME transit time to 1 AU of $\sim$ 4.3 days (corresponding to a transit speed $\sim$ 400 km/s) that is independent of CME speed is predicted (see Figure 6 of *Gopalswamy et al.* [2001]). The observations in Figure 5 suggest that the *disturbance* transit speeds range over $\sim$ 400 – 800 km/s for similar CME speeds. Thus, the *Gopalswamy et al.* [2001] $\sim$ 4.3 day prediction should not be assumed to give (and generally overestimates) the time taken for relatively slow CMEs to produce effects at Earth.

In Table 1, we have recorded the size of the geomagnetic disturbance caused by each ICME and/or its associated 'sheath' as measured by the minimum value of the *Dst* index. Figure 6 shows the distribution of the values for minimum *Dst* as a function of time, with magnetic cloud events represented by filled circles. The solar cycle dependence of the relative occurrence of magnetic clouds noted above is readily apparent, being more dominant in 1996-97 than in later years. Although some large storms are caused by ICMEs that are *not* magnetic clouds, relative to their overall numbers, magnetic clouds are responsible for a disproportionate fraction of the largest storms, most likely because by definition, they include stronger than average fields, as well as large rotations in field direction which may give rise to intervals of southward magnetic fields that drive geomagnetic activity. Another feature of Figure 6 is the general absence of strong storms in 1999. In addition to there being fewer ICMEs in this year, their magnetic field strengths were also on average weaker (see Table 2). This helps to account for the slightly lower fraction (50%) of the full halo CMEs which impacted the Earth that produced strong storms (Dst<-50) in this year compared with $\sim$80% in other years. Finally, we note the tendency for the strongest storms to occur following solar maximum.

6. Summary

We have prepared a comprehensive list of ICMEs recorded near Earth during the period 1996 through November 2002. We find that:

(a) The rate of ICMEs increased by about an order of magnitude from solar minimum to solar maximum but only approximately followed solar activity variations as indicated by the 10 cm flux (or sunspot number). The ICME rate is $\sim$ 3% of the CME rate observed by LASCO;

(b) The fraction of ICMEs that have well-organized, flux-rope-like magnetic field structures (magnetic clouds) decreased from $\sim$ 100% at solar minimum to $\sim$ 15% around solar maximum and may be recovering as activity declines. Relative to their numbers, magnetic clouds are responsible for a disproportionate fraction of major geomagnetic storms.

(c) The fastest disturbances and strongest geomagnetic storms related to ICMEs tend to occur after solar maximum;

(d) The vast majority of energetic ICMEs originated from solar events located within $\sim$ 50° of central meridian. However, there is an asymmetry in the source region distribution suggesting that sometimes CMEs form or propagate to the east of the associated active region;

(e) The ICME rate shows a $\sim$165–day periodicity that may be consistent with the "$\sim$ 154-day" periodicity previously reported in various solar data sets.

Acknowledgments.
We are indebted to the many experimenters who have made their data publicly available via the NSSDC, the ACE Science Centers and other sources. In particular, we acknowledge the use of ACE data from the MAG and SWEPAM experiments, and data from the NSSDC OMNI data-base. We also acknowledge the work of the LASCO observers Chris St Cyr, Simon Plunkett and Gareth Lawrence in preparing halo CME broadcasts and identifying frontside events. H.V.C. was supported at GSFC by a contract with USRA. I.G.R. was supported by NASA grant NCC 5-180.

References

Bame, S. J., J. R. Asbridge, W. C. Feldman, E. E. Fenimore, and J. T. Gosling, Solar wind heavy ions from flare-heated coronal plasma, *Sol. Phys., 62*, 179, 1979.

Barnden, L. R., The large-scale magnetic configuration associated with Forbush decreases, *Proc. 13th Int. Cosmic Ray Conf., 2*, 1277, 1972.

Borrini, G., J. T. Gosling, S. J. Bame, and W. C. Feldman, Helium abundance enhancements in the solar wind, *J. Geophys. Res., 87*, 7370, 1982.

Burlaga, L. F., and K. W. Ogilvie, Solar wind temperature and speed, *J. Geophys. Res., 78*, 2028, 1973.

Burlaga, L. F., E. Sittler, F. Mariani, and R. Schwenn, Magnetic loop behind an interplanetary shock: Voyager, Helios and Imp-8 observations, *J. Geophys. Res., 86*, 6673, 1981.

Burlaga, L.F., F. B. McDonald, N. F. Ness, R. Schwenn, A. J. Lazarus, and F. Mariani, Interplanetary flow systems associated with cosmic-ray modulation in 1977-1980, *J. Geophys. Res., 89*, 6579, 1984.

Burlaga, L. F., S. P. Plunkett, and O. C. St. Cyr, Successive CMEs and complex ejecta, *J. Geophys. Res., 107*, NO. A10, 1266, doi:10.1029/2001JA000255, 2002.

Brueckner, G. E. and 14 others, The large angle spectroscopic coronagraph (LASCO), *Solar Phys., 162*, 357, 1995.

Cane, H. V., The evolution of interplanetary shocks, *J. Geophys. Res., 90*, 191, 1985.

Cane, H. V., The large-scale structure of flare-associated interplanetary shocks, *J. Geophys. Res., 93*, 1, 1988.

Cane, H. V. and I. G. Richardson, Cosmic ray decreases and solar wind disturbances during late October 1989, *J. Geophys. Res., 100*, 1755, 1995.

Cane, H. V., I. G. Richardson, T. T. von Rosenvinge, and G. Wibberenz, Cosmic ray decreases and shock structure: A multispacecraft study, *J. Geophys. Res., 99*, 21,429, 1994.

Cane, H. V., I. G. Richardson, and T. T. von Rosenvinge, Cosmic ray decreases: 1964-1994, *J. Geophys. Res., 101*, 21,561, 1996.

Cane, H. V., G. Wibberenz, and I. G. Richardson, Helios 1 and 2 observations of particle decreases, ejecta and magnetic clouds, *J. Geophys. Res., 102*, 7075, 1997.

Cane, H. V., I. G. Richardson, and O. C. St. Cyr, The interplanetary events of January-May, 1997 as inferred from energetic particle data, and their relationship with solar events, *Geophys. Res. Lett., 25*, 2517, 1998a.

Cane, H. V., I. G. Richardson, and T. T. von Rosenvinge, Interplanetary magnetic field periodicity of $\sim$153 days, *Geophys. Res. Lett., 25*, 4437, 1998b.

Cane, H. V., I. G. Richardson, and O. C. St. Cyr, Coronal mass ejections, interplanetary ejecta, and geomagnetic storms, *Geophys. Res. Lett., 27*, 3591, 2000.

Cliver, E. W., J. D. Mihalov, N. R. Sheeley, R. A. Howard, M. J. Koomen, and R. Schwenn, Solar-activity and heliosphere-wide cosmic ray modulation in mid-1982, *J. Geophys. Res., 92*, 8487, 1987.

Cliver, E. W., J. Feynman, and H. B. Garrett, An estimate of the maximum speed of the solar wind, 1938-1989, *J. Geophys. Res., 103*, 17,103, 1990.

Crooker, N. U., J. T. Gosling, E. J. Smith, and C. T. Russell, A bubblelike coronal mass ejection flux rope in the solar wind, in *Physics of Magnetic Flux Ropes, Geophys. Monogr. Ser.*, vol. 58, eds. C. T. Russell, E. R. Priest, and L. C. Lee, AGU., Washington DC, 365, 1990.

Dalla, S., A. Balogh, B. Heber, and C. Lopate, Further indications of a ~140 day recurrence in energetic particle fluxes at 1 and 5 AU from the Sun, *J. Geophys. Res., 106*, 5721, 2001.

Dere, K. P., G. E. Brueckner, R. A. Howard, D. J. Michels, and J. P. Delaboudiniere, LASCO and EIT observations of helical structure in coronal mass ejections, *Astrophys. J., 516*, 465, 1999.

Fenimore, E. E., Solar wind flows associated with hot heavy ions, *Astrophys. J., 235*, 245, 1980.

Gopalswamy, N., A. Lara, R. P. Lepping, M. L. Kaiser, D. Berdichevsky, and O. C. St. Cyr, Interplanetary acceleration of coronal mass ejections, *Geophys. Res. Lett., 27*, 145, 2000.

Gopalswamy, N., A. Lara, S. Yashiro, M. L. Kaiser, R. A. Howard, Predicting the 1-AU arrival times of coronal mass ejections, *J. Geophys. Res., 106*, 29,207, 2001.

Gosling, J. T., Coronal mass ejections and magnetic flux ropes in interplanetary space, in *Physics of Magnetic Flux Ropes, Geophys. Monogr. Ser.*, vol. 58, edited by C. T. Russell, E. R. Priest, and L. C. Lee, p. 343, AGU, Washington, D. C., 1990.

Gosling, J. T., V. Pizzo, and S. J. Bame, Anomalously low proton temperatures in the solar wind following interplanetary shock waves - Evidence for magnetic bottles?, *J. Geophys. Res., 78*, 2001, 1973.

Gosling, J. T., D. N. Baker, S. J. Bame, W. C. Feldman, R. D. Zwickl, and E. J. Smith, Bidirectional solar wind electron heat flux events, *J. Geophys. Res., 92*, 8519, 1987.

Gosling, J. T., J. Birn, and M. Hesse, Three-dimensional magnetic reconnection and the magnetic topology of coronal mass ejection events, *Geophys. Res. Lett., 22*, 869, 1995.

Gosling, J. T., R. M. Skoug, and W. C. Feldman, Solar wind electron halo depletions at 90° pitch angle, *Geophys. Res. Lett., 28*, 4155, 2001.

Hirshberg, J., S. J. Bame, and D. E. Robbins, Solar flares and solar helium enrichments: July 1965-July 1967, *Sol. Phys., 23*, 467, 1972.

Ipavich, F. M., A. B. Galvin, G. Gloeckler, D. Hovestadt, S. J. Bame, B. Klecker, M. Scholer, L. A. Fisk, and C. Y. Fan, Solar wind Fe and CNO measurements in high-speed flows, *J. Geophys. Res., 91*, 4133, 1986.

Lepping, R. P., J. A. Jones, and L. F. Burlaga, Magnetic field structure of interplanetary magnetic clouds at 1 AU, *J. Geophys. Res., 95*, 11,957, 1990.

Lepri, S. T., T. H. Zurbuchen, L. A. Fisk, I. G. Richardson, H. V. Cane, and G. Gloeckler, Iron charge distribution as an identifier of interplanetary coronal mass ejections, *J. Geophys. Res., 106*, 29,231, 2001.

Lopez, R. E., Solar cycle invariance in solar wind proton temperature relationships, *J. Geophys. Res., 92*, 11,189, 1987.

Luhmann, J. G., Y. Li, C. N. Arge, P. Gazis, and R. Ulrich, Solar cycle changes in coronal holes and space weather cycles, *J. Geophys. Res., 107*, 10.1029/2001JA007550, 2002.

Marsden, R. G., T. R. Sanderson, C. Tranquille, K.-P. Wenzel, and E. J. Smith, ISEE 3 observations of low-energy proton bidirectional events and their relation to isolated interplanetary magnetic structures, *J. Geophys. Res., 92*, 11,009, 1987.

McGuire, R. E., T. T. von Rosenvinge, and F. B. McDonald, The composition of solar energetic particles, *Astrophys. J., 301*, 938, 1986.

Mitchell, D. G., E. C. Roelof, and S. J. Bame, Solar wind iron abundance variations at speeds > 600 km sec^{-1}, 1972-1976, *J. Geophys. Res., 88*, 9059, 1983.

Montgomery, M. D., J. R. Asbridge, S. J. Bame, and W. C. Feldman, Solar wind electron temperature depressions following some interplanetary shock waves: evidence for magnetic merging?, *J. Geophys. Res., 79*, 3103, 1974.

Morrison, P., Solar origin of cosmic ray time variations, *Phys. Rev., 101*, 1397, 1956.

Neugebauer, M., and R. Goldstein, Particle and field signatures of coronal mass ejections in the solar wind, in *Coronal Mass Ejections*, eds. N. Crooker, J. A. Joselyn, and J. Feynman, AGU., Washington DC, 245, 1997.

Neugebauer M., J. T. Steinberg, R. L. Tokar, B. L. Barraclough, E. E. Dors, R. C. Wiens, D. E. Gingerich, D. Luckey, and D. B. Whiteaker, Genesis on-board determination of the solar wind flow regime, *Space Sci. Rev.*, in press, 2002.

Osherovich, V., and L. F. Burlaga, Magnetic clouds, in *Coronal Mass Ejections*, eds. N. Crooker, J. A. Joselyn, and J. Feynman, AGU., Washington DC, 157, 1997.

Palmer, I. D., F. R. Allum, and S. Singer, Bidirectional anisotropies in solar cosmic ray events: Evidence for magnetic bottles, *J. Geophys. Res., 83*, 75, 1978.

Richardson, I. G., and H. V. Cane, Signatures of shock drivers in the solar wind and their dependence on the solar source location, *J. Geophys. Res., 98*, 15,295, 1993.

Richardson, I. G., and H. V. Cane, Regions of abnormally low proton temperature in the solar wind (1965-1991) and their association with ejecta, *J. Geophys. Res., 100*, 23,397, 1995.

Richardson, I. G., and H. V. Cane, Particle flows observed in ejecta during solar event onsets and their implication for the magnetic field topology, *J. Geophys. Res., 101*, 27,521, 1996.

Richardson, I. G., and D. V. Reames, Bidirectional ~ 1 MeV ion intervals in 1973-1991 observed by the Goddard Space Flight Center instruments on IMP 8 and ISEE 3/ICE, *Astrophys. J. Suppl. Ser., 85*, 411, 1993.

Richardson, I. G., H. V. Cane, and T. T. von Rosenvinge, Prompt arrival of solar energetic particles from far eastern events: The role of large-scale interplanetary magnetic field structure, *J. Geophys. Res., 96*, 7853, 1991.

Richardson, I. G., H. V. Cane, and O. C. St. Cyr, Relationships between coronal and interplanetary structures inferred from energetic particle observations, in *Solar Wind Nine*, edited by S. R. Habbal et al., *AIP Conf. Proc., 471*, 677, 1999.

Richardson, I. G., V. M. Dvornikov, V. E. Sdobnov., and H. V. Cane, Bidirectional particle flows at cosmic ray and lower (~ 1 MeV) energies and their association with interplanetary coronal mass ejections/ejecta, *J. Geophys. Res., 105*, 12,597, 2000.

Richardson, I. G., E. W. Cliver, and H. V. Cane, Sources of geomagnetic storms for solar minimum and maximum conditions during 1972-2000, *Geophys. Res. Lett., 28*, 2569, 2001a.

Richardson, I. G., V. M. Dvornikov, V. E. Sdobnov, and H. V. Cane, Bidirectional cosmic ray and ~ 1 MeV ion flows, and their association with ejecta, *Proc. 27^{th} Int. Cosmic Ray Conf., 9*, 3498, 2001b.

Richardson, I. G., H. V. Cane, and E. W. Cliver, Sources of geomagnetic activity during nearly three solar cycles (1972-2000), *J. Geophys. Res., 107*, 10.1029/2001JA000504, 2002.

Sheeley, N. R., Jr., R. A. Howard, M. J. Koomen, D. J. Michels, R. Schwenn, K. H. Mühlhäser, and H. Rosenbauer, Coronal mass ejections and interplanetary shocks, *J. Geophys. Res., 90*, 163, 1985.

Sheeley, N. R., Jr., W. N. Hakala, and Y.-M. Wang, Detection of coronal mass ejection associated shock waves in the outer corona, *J. Geophys. Res., 105*, 5081, 2000.

St. Cyr, O. C., and 14 others, Properties of coronal mass ejections: SOHO LASCO observations from January 1996 to June 1998, *J. Geophys. Res., 105*, 18,169, 2000.

Wang, Y. M., P. Z. Ye, S. Wang, G. P. Zhou, and J. X. Wang, A statistical study on the geoeffectiveness of Earth-directed coronal mass ejections from March 1997 to December 2000,*J. Geophys. Res., 107*, 10.1029/2002JA009244, 2002.

Webb, D. F., and R. A. Howard, The solar cycle variation of coronal mass ejections and the solar wind mass flux, *J. Geophys. Res., 99*, 4201, 1994.

Webb, D. F., E. W. Cliver, N. U. Crooker, O. C. St. Cyr, and B. J. Thompson, The relationship of halo CMEs, magnetic clouds and magnetic storms, *J. Geophys. Res., 105*, 7,491, 2000.

Woo, R., J. W. Armstrong, N. R. Sheeley, Jr., R. A. Howard, M. J. Koomen, D. J. Michels, and R. Schwenn, Doppler scintillation observations of interplanetary shocks within 0.3 AU, *J. Geophys. Res., 90*, 154, 1985.

Zhao, X. P., and D. F. Webb, The source regions and storm–effectiveness of frontside full halo coronal mass ejections, *J. Geophys. Res.*,, in press, 2002.

Zwickl, R. D., J. R. Asbridge, S. J. Bame, W. C. Feldman, and J. T. Gosling, He^+ and other unusual ions in the solar wind: A systematic search covering 1972-1980, *J. Geophys. Res., 87*, 7379, 1982.

Zwickl, R. D., J. R. Asbridge, S. J. Bame, W. C. Feldman, J. T. Gosling, and E. J. Smith, Plasma properties of driver gas following interplanetary shocks observed by ISEE-3, in *Solar Wind Five; NASA Conference Proceedings 2280*, edited by M. Neugebauer, p. 711, NASA, Washington, DC, 1983.

H. V. Cane and I. G. Richardson, Laboratory for High Energy Astrophysics, Code 661, NASA Goddard Space Flight Center, Greenbelt, MD, 20771 (hilary.cane@utas.edu.au; richardson@lheavx.gsfc.nasa.gov)

(Received _____.)

Table 1. Near-Earth ICMEs in 1996-1997

Disturbance Time[a] (UT)	ICME Start (UT)	ICME End (UT)	Qual.[b]	SC[c] (γ)	V_{ej} (km/s)	V_{max} (km/s)	B (nT)	MC?	Dst (nT)	V_{tr} (km/s)	LASCO CME[d]
1996											
May 27 1500	May 27 1500	May 29 0000	2	...	370	400	9	2	-33	...	
July 01 1320	July 01 1800	July 02 1100	2	0	360	370	10	2	-20	...	
Aug. 07 1300	Aug. 07 1300	Aug. 08 1000	2	...	350	380	7	2	-23	...	
Dec. 23 1600	Dec. 23 1700	Dec. 25 1000	2	...	360	420	10	2	-18	480	Dec. 19 1630 H
1997											
Jan. 10 0104	Jan. 10 0400	Jan. 11 0200	1	9	450	460	14	2	-78	507	Jan. 06 1510 H
Feb. 09 1321	Feb. 10 0200	Feb. 10 1900	1	22	450	600	8	2	-68	681	Feb. 07 0030 H
Feb. 16 1600	Feb. 16 2300	Feb. 17 1800	1	...	350	350	9	1	-54	...	
April 10 1745	April 11 0600	April 11 2000	1	0	430	420	22	0	-82	552	April 07 1427 H
April 21 0600	April 21 1000	April 23 0400	2	...	400	400	12	2	-107	...	
May 15 0159	May 15 0900	May 16 0000	1	33	450	430	23	2	-115	610	May 12 0630 H
May 26 0957	May 26 1600	May 27 1000	2	2	350	350	10	1	-74	381	May 21 2100
June 08 1636	June 08 1800	June 10 0000	2	0	380	400	12	2	-84	...	
June 19 0032	June 19 0700	June 20 2300	2	0	360	390	8	2	-36	...	
July 15 0311	July 15 0800	July 16 1100	1	0	350	360	12	2	-45	...	
Aug. 03 1042	Aug. 03 1300	Aug. 04 0300	1	0	400	480	16	2	-48	400	July 30 0445 H
Aug. 17 0200	Aug. 17 0600	Aug. 17 2000	1	...	390	410	7	0	-28	...	
Sept. 03 0800	Sept. 03 1300	Sept. 03 2100	1	...	400	490	15	0	-98	390	Aug. 30 0130 H
Sept. 17 0800	Sept. 17 1600	Sept. 18 0200	1	...	330	350	8	2	-45	...	
Sept. 21 1651	Sept. 21 2100	Sept. 22 1600	1	0	450	470	20	2	-36	440	Sept. 17 2028 H
Oct. 01 0059	Oct. 01 1600	Oct. 02 2300	2	23	450	470	10	2	-98	580	Sept. 28 0108 H
Oct. 10 1612	Oct. 10 2200	Oct. 12 0000	1	15	400	450	12	2	-130	400	Oct. 06 1528
Oct. 26 1200	Oct. 27 0000	Oct. 28 0700	2	...	500	520	7	1	-60	470	Oct. 23 1126 H
Nov. 06 2248	Nov. 07 0400	Nov. 09 1200	1	33	400	460	15	2	-11	640	Nov. 04 0610 H
Nov. 22 0949	Nov. 22 1500	Nov. 23 1400	2	34	510	510	17	2	-108	600	Nov. 19 1227 H
Dec. 10 0526	Dec. 10 1800	Dec. 12 0000	1	32	350	380	15	0	-60	460	Dec. 06 1027
Dec. 30 0209	Dec. 30 1200	Dec. 31 1100	3	11	390	360	12	1	-77	430	Dec. 26 0231

[a] The time of the associated SC when present. Otherwise, 'A' indicates the time of shock passage at ACE. If no shock or SC is reported, the estimated arrival time of the disturbance (which in some cases is also the ICME leading edge) is given to the nearest hour.

[b] The quality of the boundary times ('1' indicating the most reliable).

[c] The SC size is the mean horizontal component for mid-latitude stations (from reports in *Solar-Geophysical Data*).

[d] 'H' indicates that the CME had a 360° angular extent (i.e. halo CME). '?' indicates that the CME association may be doubtful. Times in brackets indicate associated solar events during an interval with no coronagraph coverage. 'dg' indicates that there was a LASCO data gap around the expected time of the associated CME.

[e] ICMEs could result from multiple CMEs.

Figure 1. Plot of maximum solar wind speed (V_{max}) associated with an ICME versus the transit speed of the disturbance from the Sun to the Earth. The lower limit to V_{max} for a particular transit speed permits some potential CME–ICME associations to be ruled out.

Figure 2. (a) Three-Carrington-rotation running mean of the ICME rate (number of ICMEs/solar rotation) in 1996-2002. (b) Carrington-rotation average 10 cm flux of the Sun. Note that the 10 cm flux increases more uniformly than the ICME rate and in particular does not show a significant decrease in 1999.

Figure 3. Transit speeds of the shocks/disturbances associated with those ICMEs that can be related to CMEs observed by the LASCO coronagraphs (or with a solar event if LASCO observations are not available). Note that more events with speeds greater than 1000 km/s (indicated by the dashed horizontal line) occur after solar maximum in early 2000 (indicted by the dashed vertical line) than before this time.

Figure 4. Distribution of the longitudes of the solar chromospheric events associated with ICMEs at the Earth.

Figure 5. Distribution of disturbance transit speeds as a function of the sky–plane speeds of the associated CMEs.

Figure 6. Distribution of minimum geomagnetic *Dst* values during the passage of the ICMEs or the related sheath regions as a function of time. The filled circles represent events that were magnetic clouds. Although these generally produce stronger geomagnetic effects, not all strong ICME–related storms result from magnetic clouds. Note that a larger fraction of ICMEs are magnetic clouds in 1996 and 1997.

Table 2. Near-Earth ICMEs in 1998-1999

Disturbance Time[a] (UT)	ICME Start (UT)	ICME End (UT)	Qual.[b]	SC[c] (γ)	V_{ej} (km/s)	V_{max} (km/s)	B (nT)	MC?	Dst (nT)	V_{tr} (km/s)	LASCO CME[d]
1998											
Jan. 06 1416	Jan. 07 0100	Jan. 08 2200	2	29	400	410	16	2	-83	480	Jan. 02 2328 H
Jan. 09 0700	Jan. 09 0700	Jan. 10 0800	2	...	450	500	6	0	-45	...	
Jan. 20 0000	Jan. 20 1700	Jan. 21 0400	2	...	430	450	5	1	-42	...	
Jan. 21 0400	Jan. 21 0600	Jan. 22 1300	3	...	380	400	12	0	-27	430	Jan. 17 0409 H
Jan. 29 1800	Jan. 29 1400	Jan. 31 0100	2	...	350	400	7	0	-72	430	Jan. 25 1526 H
Feb. 04 0000	Feb. 04 0400	Feb. 05 2300	1	...	320	390	11	2	-50	...	
Feb. 17 0400	Feb. 17 1000	Feb. 17 2100	2	...	400	400	12	1	-102	602	Feb. 14 0655
Feb. 18 0750(A)	Feb. 18 2300	Feb. 20 0000	2	...	440	460	9	1	-66	...	
March 04 1156	March 04 1300	March 06 0900	1	0	350	380	12	2	-56	430	Feb. 28 1248
March 06 0300	March 06 1500	March 07 1600	1	...	330	330	7	1	-25	...	
March 25 1000	March 25 1300	March 26 1000	1	...	400	400	10	0	-72	...	
April 11 2300	April 11 2300	April 13 1800	3	...	390	390	8	0	-56	...	
May 01 2156	May 02 0500	May 03 1700	2	29	520	650	10	2	-100	780	April 29 1658 H
May 04 0215(A)	May 04 1000	May 08 0000	3	...	550	780	12	0	-216	1120	May 02 1406 H[e]
May 15 1451	May 15 2300	May 16 0800	2	0	400	340	15	0	-14	...	
May 29 1536	May 29 2200	May 30 1600	3	0	700	700	10	1	-58	...	
June 02 0800	June 02 1000	June 02 1800	2	...	390	400	11	2	-14	...	
June 13 1925	June 14 0400	June 15 0600	2	0	350	400	11	1	-68	...	
June 24 1000	June 24 1300	June 25 2100	2	...	450	540	13	2	-33	...	June 21 0535?
June 25 1636	June 26 0000	June 26 1900	1	0	460	490	10	0	-111	...	
July 05 0500	July 06 0600	July 09 0700	1	...	450	630	5	0	-37	...	dg
July 10 2300	July 11 0000	July 13 1500	2	...	400	400	10	0	-45	...	dg
July 30 2333	July 31 0600	July 31 1600	3	0	410	430	13	1	-51	...	dg
Aug. 01 0400	Aug. 01 0400	Aug. 03 0300	3	...	410	450	7	1	-30	...	dg
Aug. 05 1300	Aug. 05 1300	Aug. 06 1200	2	...	360	420	13	1	-166	...	dg
Aug. 07 1800	Aug. 07 2300	Aug. 09 2300	2	...	450	500	7	0	-73	...	dg
Aug. 10 0046	Aug. 10 1100	Aug. 11 0800	3	11	400	500	8	0	-37	...	dg
Aug. 11 2300	Aug. 12 0100	Aug. 13 1400	3	...	380	420	7	1	-28	...	dg
Aug. 19 1847	Aug. 20 0600	Aug. 21 2000	1	0	300	340	14	2	-86	...	dg
Aug. 26 0651	Aug. 26 2200	Aug. 28 0000	2	53	650	860	14	0	-188	1260	dg (Aug. 24 2200)
Sept. 24 2345	Sept. 25 0600	Sept. 26 1600	1	45	620	770	20	2	-234	1150	dg (Sept. 23 1100)
Oct. 18 1952	Oct. 19 0400	Oct. 20 0700	2	22	400	410	18	2	-139	507	Oct. 15 1004 H
Oct. 23 1230(A)	Oct. 23 1900	Oct. 25 1000	3	...	500	600	5	0	-60	...	
Nov. 07 0815	Nov. 07 2200	Nov. 08 1200	2	13	450	530	15	1	-92	550	Nov. 04 0418 H
Nov. 08 0451	Nov. 08 1900	Nov. 10 2000	2	0	450	640	12	2	-148	730	Nov. 05 2044 H
Nov. 13 0143	Nov. 13 0200	Nov. 14 1200	2	0	390	400	17	0	-134	520	Nov. 09 1818
Nov. 30 0507	Nov. 30 0900	Dec. 01 0600	3	24	400	470	8	0	0	...	
Dec. 28 1826	Dec. 29 1800	Dec. 31 0200	2	11	400	410	8	0	-53	...	dg
1999											
Jan. 04 0000	Jan. 04 0400	Jan. 04 2200	3	...	350	360	8	0	-28	...	dg
Jan. 13 1054	Jan. 13 1500	Jan. 13 2200	2	18	420	420	20	0	-113	...	dg
Jan. 22 1950(A)	Jan. 23 0900	Jan. 24 0200	3	...	530	670	12	0	-49	...	dg
Feb. 13 1900	Feb. 13 1900	Feb. 14 1500	3	dg	440	470	9	0	-22	...	
Feb. 18 0246	Feb. 18 1000	Feb. 21 0000	2	41	520	700	8	2	-134	870	dg (Feb. 16 0312)
March 10 0130	March 10 1700	March 12 1200	2	8	410	460	7	0	-78	...	
April 16 1125	April 16 1800	April 17 1900	1	18	400	450	20	2	-105	520	April 13 0330 H
April 20 1600	April 21 0400	April 22 1600	1	...	500	620	8	1	-32	...	April 18 0830?
May 15 1600	May 15 1600	May 18 0000	2	...	390	400	5	0	-10	...	
June 02 2000	May 23 1800	May 24 2200	2	...	430	470	9	1	-6	...	
June 26 0325	June 26 0600	June 26 1900	3	8	350	350	15	1	-20	530	June 22 1854 H
June 26 2016	June 27 1400	June 28 1400	3	36	680	880	8	0	-43	760	June 24 1331 H
July 02 0059	July 02 2200	July 06 0600	2	11	450	650	5	0	-34	...	
July 06 1509	July 06 2100	July 08 0400	3	15	440	450	5	1	-8	620	July 03 1954
July 27 0000	July 27 1700	July 29 0600	3	...	390	430	6	0	-40	540	July 23 2130
July 30 1600	July 30 2000	July 31 0800	3	...	500	660	8	1	-60	710	July 28 0530? H
July 31 1837	July 31 1900	Aug. 02 0600	3	17	480	650	5	1	-37	497	July 28 0906 H
Aug. 02 1100	Aug. 02 1400	Aug. 03 1100	3	...	370	400	4	0	-21	...	
Aug. 08 1841	Aug. 08 1900	Aug. 10 1700	2	0	360	420	9	2	-62	...	
Aug. 11 2300	Aug. 12 2000	Aug. 14 0000	3	...	370	420	7	0	-24	615	Aug. 09 0326
Aug. 20 2300	Aug. 20 2300	Aug. 23 1600	2	...	450	570	8	1	-80	510	Aug. 17 1331
Sept. 22 1222	Sept. 22 1900	Sept. 24 1800	1	36	510	600	10	0	-164	700	Sept. 20 0606 H
Oct. 21 0225	Oct. 21 0800	Oct. 22 0700	2	42	500	580	20	0	-231	480	Oct. 18 0026 H
Nov. 11 1900	Nov. 12 1000	Nov. 13 1800	1	...	450	680	5	0	-100	...	dg
Nov. 22 0000	Nov. 22 0000	Nov. 24 0300	3	...	450	490	9	0	-38	...	dg
Dec. 12 1551	Dec. 12 1900	Dec. 13 1600	2	16	520	700	12	0	-92	...	dg
Dec. 13 2300	Dec. 14 0400	Dec. 14 2000	2	...	440	480	12	0	-37	...	dg
Dec. 26 2130(A)	Dec. 27 1100	Dec. 28 0400	2	...	430	450	8	1	-9	...	

Table 3. Near-Earth ICMEs in 2000

Disturbance Time[a] (UT)	ICME Start (UT)	ICME End (UT)	Qual.[b]	SC[c] (γ)	V_{ej} (km/s)	V_{max} (km/s)	B (nT)	MC?	Dst (nT)	V_{tr} (km/s)	LASCO CME[d]
2000											
Jan. 18 1500	Jan. 19 0300	Jan. 19 1500	2	...	270	330	7	0	-5	...	
Jan. 22 0023	Jan. 22 1700	Jan. 23 0200	2	...	380	415	16	1	-91	530	Jan. 18 1754 H
Feb. 11 0258	Feb. 11 1600	Feb. 11 2000	1	0	420	505	7	0	-25	630	Feb. 08 0930 H
Feb. 11 2352	Feb. 12 1200	Feb. 13 0000	2	49	540	590	13	1	-169	900	Feb. 10 0230 H
Feb. 14 0731	Feb. 15 0000	Feb. 16 0800	3	0	500	686	5	0	-88	730	Feb. 12 0431 H
Feb. 20 2139	Feb. 21 0500	Feb. 22 1400	2	24	400	460	16	2	-20	570	Feb. 17 2006 H
March 01 0130	March 01 0300	March 02 0300	1	...	480	530	8	0	-49	...	
March 09 2300	March 10 0100	March 10 0600	2	...	390	400	6	1	0	...	
March 18 2200	March 19 0200	March 19 1200	1	...	380	390	9	0	-2	...	
March 29 1100	March 29 1900	March 31 2300	2	...	420	590	6	0	-58	...	
April 06 1639	April 07 0700	April 08 1800	2	74	550	620	5	1	-321	870	April 04 1632 H
April 24 0400	April 24 0400	April 24 1400	2	...	490	520	13	0	-7	...	
April 27 1800	April 27 1800	April 28 0100	1	...	400	410	10	1	-15	...	
May 02 1045(A)	May 02 2000	May 05 1000	3	...	500	860	6	0	-38	...	April 29 0154?
May 06 1600	May 07 0000	May 08 1600	3	...	380	440	10	0	-4	...	
May 13 1700	May 13 1700	May 14 1800	2	...	500	600	8	0	0	603	May 10 2006
May 15 1900	May 15 1900	May 16 1200	3	...	430	450	8	0	-25	...	
May 16 2300	May 16 2300	May 17 0700	2	...	550	580	9	1	-88	500	May 13 1226
May 23 0700	May 23 1000	May 23 2100	2	...	570	610	12	0	0	650	May 20 1450
May 23 2300	May 24 1200	May 26 1600	2	...	550	690	5	1	-147	653	
June 04 1502	June 05 0000	June 06 2200	3	17	470	560	10	1	-35	403	May 31 0806
June 08 0910	June 08 1600	June 10 1700	3	59	550	790	10	0	-87	1100	June 06 1554 H
June 11 0801	June 11 0700	June 11 1800	2	0	510	530	11	1	-41	...	
June 12 2208	June 13 1200	June 14 0600	2	0	440	550	7	0	-39	...	
June 18 0900	June 18 0900	June 18 1700	2	...	380	400	6	1	-9	...	
June 23 1303	June 24 0200	June 26 0800	2	37	500	590	8	0	-33	...	
June 26 0000	June 26 1000	June 27 0000	1	...	540	560	10	0	-74	...	
June 30 0700	June 30 0700	June 30 2300	2	...	380	400	6	0	-6	...	
July 01 0100	July 01 0600	July 03 0800	3	...	390	440	7	1	0	...	
July 10 0638	July 11 0200	July 11 1400	2	36	440	490	13	0	0	609	July 07 1026 H
July 11 1123(A)	July 11 2200	July 13 0200	1	...	520	540	10	1	-24	...	
July 13 0942	July 13 1600	July 14 1500	2	31	620	700	7	0	-35	940	July 11 1327 H
July 14 1532	July 14 1700	July 15 1400	2	29	780	800	9	1	-60	...	July 12 2030?
July 15 1437	July 15 1900	July 17 0800	2	120	850	980	20	2	-300	1600	July 14 1054 H
July 19 1527	July 20 0100	July 21 0700	2	19	530	630	8	0	-95	...	July 17 0854?
July 23 1041	July 23 1500	July 25 0400	3	0	380	430	9	0	-66	...	dg
July 26 1857	July 27 0200	July 28 0200	2	0	360	400	6	1	-43	490	July 23 0530
July 28 0634	July 28 1200	July 30 1300	3	45	460	480	10	2	-74	580	July 25 0330 H
Aug. 10 0407(A)	Aug. 10 1900	Aug. 11 2100	1	...	430	490	12	1	-103	...	Aug. 06 1830?
Aug. 11 1845	Aug. 12 0500	Aug. 13 2200	1	21	580	670	16	2	-237	810	Aug. 09 1630 H
Sept. 02 1300	Sept. 02 2200	Sept. 03 1300	1	...	430	450	8	0	-58	...	Aug. 29 1830?
Sept. 08 1200	Sept. 08 1800	Sept. 10 1000	2	...	450	500	5	0	-44	530	Sept. 05 0554
Sept. 17 1657(A)	Sept. 17 2300	Sept. 21 0000	3	...	600	880	10	2	-172	...	Sept. 15/16[e]
Oct. 03 0054	Oct. 03 1000	Oct. 05 0300	1	0	400	430	14	2	-146	...	
Oct. 05 0326	Oct. 05 1300	Oct. 07 1100	2	0	450	530	6	1	-192	580	Oct. 02 2026 H
Oct. 12 2228	Oct. 13 0800	Oct. 14 1700	2	21	410	470	13	2	-110	580	Oct. 09 2350 H
Oct. 20 1800	Oct. 20 2200	Oct. 21 0800	1	...	400	440	4	0	-2	...	
Oct. 28 0954	Oct. 28 2100	Oct. 29 2200	2	35	380	420	14	2	-113	616	Oct. 25 0826 H
Nov. 06 0948	Nov. 06 2200	Nov. 08 0300	3	18	510	610	20	2	-159	...	
Nov. 10 0628	Nov. 10 1000	Nov. 11 0400	2	86	850	930	8	0	-104	1400	Nov. 08 2306 H
Nov. 11 0400(A)	Nov. 11 0800	Nov. 12 0000	2	...	790	910	7	0	-43	1200	(Nov. 09 1615)
Nov. 26 1158	Nov. 27 0800	Nov. 28 0300	2	0	580	630	11	0	-72	...	Nov. 24 [e]
Nov. 28 0530	Nov. 28 1600	Nov. 29 1900	2	24	530	590	10	1	-130	720	Nov. 25/26[e]

Table 4. Near-Earth ICMEs in 2001-2002

Disturbance Time[a] (UT)	ICME Start (UT)	ICME End (UT)	Qual.[b]	SC[c] (γ)	V_{ej} (km/s)	V_{max} (km/s)	B (nT)	MC?	Dst (nT)	V_{tr} (km/s)	LASCO CME[d]
2001											
Jan. 23 1048	Jan. 24 0900	Jan. 26 0800	1	30	400	550	5	1	-55	680	Jan. 20 2130 H[e]
March 03 1121	March 04 0400	March 05 0200	2	0	440	520	8	0	-71	610	Feb. 28 1450
March 19 1114	March 19 1700	March 21 2200	1	19	410	490	17	2	-165	520	March 16 0350
March 27 1747	March 28 0600	March 30 1900	3	26	520	650	4	0	-98	850	March 25 1706 H
March 31 0052	March 31 0500	March 31 1000	3	105	640	710	39	1	-358	690	March 28 1250 H
March 31 2200	April 01 0400	April 03 0300	2	...	640	820	5	0	0	700	March 29 1026 H
April 04 1455	April 05 1100	April 07 0300	3	57	520	780	6	0	-38	1020	April 02 2206
April 08 1101	April 08 1900	April 10 1000	3	41	610	780	8	0	-51	1050	April 06 1930 H
April 11 1343	April 11 2200	April 13 0700	2	0	640	740	14	2	-257	1220	April 10 0530 H
April 13 0734	April 13 0900	April 14 1200	1	31	730	830	9	0	-66	970	April 11 1331 H
April 18 0046	April 18 1200	April 20 1100	2	0	430	520	8	0	-100	580	
April 21 1601	April 21 2300	April 23 0800	1	19	350	390	11	2	-104	...	
April 28 0431(A)	April 28 1400	May 1 0200	2	58	540	730	8	2	-33	1080	April 26 1230 H
May 07 0800	May 07 1900	May 08 0700	1	...	360	410	8	1	-24	...	
May 08 1101	May 09 1200	May 10 2200	2	...	430	560	8	1	-70	...	
May 11 1300	May 11 1300	May 12 0000	2	...	430	430	8	0	-40	...	
May 12 0920(A)	May 12 1700	May 13 1600	3	...	570	670	7	0	-46	...	May 10 0131?
May 15 1500	May 16 0900	May 17 0000	3	...	460	530	5	1	-20	...	
May 27 1459	May 28 0300	May 29 2100	1	0	460	600	8	2	-39	...	
May 30 0800	May 30 0800	May 31 0800	2	...	350	370	5	1	-2	...	
June 07 0852(A)	June 07 1800	June 08 0700	1	...	390	430	9	1	-4	...	
June 21 0300	June 21 0300	June 21 1000	3	...	570	600	5	1	-27	...	
June 26 1200	June 27 0300	June 28 1700	1	...	420	490	3	0	-18	...	
July 08 1200	July 09 0200	July 11 0400	2	...	400	460	4	1	-41	520	July 05 0354
July 13 1700	July 13 1700	July 14 0100	2	...	400	420	8	1	-8	...	
Aug. 03 0716	Aug. 03 1100	Aug. 03 1400	3	0	420	440	10	0	-17	...	
Aug. 15 0500	Aug. 15 0500	Aug. 16 1400	3	...	390	450	5	0	-16	...	
Aug. 17 1103	Aug. 17 2000	Aug. 20 0000	2	29	490	600	10	0	-104	620	Aug. 14 1601 H
Aug. 27 1952	Aug. 28 2000	Aug. 29 2000	3	20	470	580	4	0	-20	810	Aug. 25 1650 H
Aug. 30 1411	Aug. 30 2000	Aug. 31 1000	2	0	420	500	6	1	-45	...	
Sept. 01 1300	Sept. 01 1300	Sept. 02 1800	2	...	360	410	5	1	-17	...	
Sept. 13 0200	Sep 13 1800	Sep 14 2200	2	...	410	440	10	1	-58	...	
Sept. 23 1100	Sept. 24 0000	Sept. 25 0000	3	...	450	570	7	1	-77	700	Sept. 20 1931
Sept. 29 0940	Sept. 30 0000	Oct. 01 0000	2	0	520	700	12	1	-64	...	Sept. 27 0454?
Sept. 30 1924	Oct. 01 0800	Oct. 02 0000	2	0	490	550	9	0	-150	710	Sept. 28 0854 H
Oct. 01 2200	Oct. 02 1200	Oct. 03 1600	2	...	510	530	13	1	-182	715	Sept. 29 1154
Oct. 11 1701	Oct. 12 0200	Oct. 12 1100	2	46	530	580	17	1	-74	770	Oct. 09 1130 H
Oct. 21 1648	Oct. 22 0000	Oct. 25 1000	1	61	470	670	9	0	-166	860	Oct. 19 1650 H
Oct. 26 2200	Oct. 27 0000	Oct. 28 0200	2	...	390	410	8	0	-28	417	Oct. 23 1826
Oct. 28 0319	Oct. 29 2200	Oct. 31 1300	2	48	360	510	4	0	-160	694	Oct. 25 1526
Oct. 31 1348	Oct. 31 1800	Nov. 02 1200	2	19	340	390	11	2	-97	...	
Nov. 06 0152	Nov. 06 2100	Nov. 09 0600	2	110	570	750	6	0	-277	1240	Nov. 04 1635 H
Nov. 19 1815	Nov. 19 2200	Nov. 20 1100	3	0	480	580	6	1	-32	680	Nov. 17 0530 H
Nov. 24 0656	Nov. 24 1400	Nov. 26 1100	2	62	660	1000	12	2	-213	1300	Nov. 22 2330 H
Nov. 27 0300	Nov. 27 0300	Nov. 27 1200	2	...	470	480	6	0	-27	...	
Dec. 28 0000	Dec. 28 0000	Dec. 29 1200	2	...	360	370	8	0	0	...	
Dec. 29 0538	Dec. 30 0000	Dec. 30 1400	2	78	400	460	17	1	-39	570	Dec. 26 0530?
2002											
Feb. 15 1000	Feb. 15 1000	Feb. 15 1700	1	...	370	380	7	1	0	621	Feb. 12 1506 H
Feb. 28 0451	Feb. 28 1700	March 01 1000	2	46	390	410	13	1	-64	...	
March 18 1322	March 19 0500	March 20 1600	2	64	380	470	15	2	-41	667	March 15 2306
March 20 1328	March 21 1400	March 22 0600	3	15	440	580	8	0	-10	...	
March 23 1137	March 23 2100	March 25 2000	2	24	450	500	15	2	-101	625	March 20 1706?
April 12 0100	April 12 0100	April 13 1300	3	...	420	450	8	0	-20	...	
April 17 1107	April 17 2100	April 19 0900	2	54	480	610	12	1	-126	...	
April 19 0835	April 20 0000	April 21 1800	2	30	500	640	8	2	-152	863	April 17 0826 H
May 20 0340	May 20 1500	May 21 2200	3	13	410	510	6	0	-33	420	May 16 0050 H
May 21 2203	May 22 1800	May 23 0500	3	17	420	440	9	0	-13	...	
May 23 1050	May 23 2000	May 25 1800	2	59	590	920	11	2	-108	1323	May 22 0326 H
July 17 1603	July 18 1200	July 19 0900	3	0	460	520	6	0	-13	955	July 15 2030 H
July 19 1450(A)	July 20 0400	July 22 0600	2	13	650	930	6	0	-33	...	
Aug. 01 0510	Aug. 01 0900	Aug. 01 2300	2	26	450	460	12	2	-46	...	
Aug. 01 2309	Aug. 02 0400	Aug. 04 0100	2	18	460	520	10	0	-85	505	July 29 1145
Aug. 18 1846	Aug. 19 1200	Aug. 21 1400	2	44	460	580	8	1	-92	777	Aug. 16 1230 H
Aug. 29 2100	Aug. 29 2100	Aug. 30 0600	2	...	400	420	8	1	-35	...	
Sept. 07 1610(A)	Sept. 08 0400	Sept. 08 2000	2	dg	470	550	10	0	-164	882	Sept. 05 1654 H
Sept. 08 2000	Sept. 08 2200	Sept. 10 2100	2	dg	440	520	9	0	-64	...	
Sept. 19 0600	Sept. 19 2000	Sept. 20 2100	2	dg	490	750	5	0	-26	901	Sept. 17 0754 H
Oct. 02 2210(A)	Oct. 03 0100	Oct. 04 1800	2	dg	430	520	11	2	-13	...	
Nov. 17 0000	Nov. 17 1000	Nov. 18 1200	2	dg	380	500	8	2	-24	...	

Table 5. Summary of Average ICME Properties

	1996 (Minimum)	1997	1998	1999	2000 (Maximum)	2001	2002	All
Number of Events	4	22	38	28	53	47	22	214
ICME Speed (km/s)	360±4	406±11	428±14	448±13	490±17	470±14	452±14	454±6
ICME Av. B (nT)	9.0±.7	12.9±1.4	10.7±0.6	9.4±0.9	9.5±0.5	8.8±0.8	9.3±0.6	9.9±0.3
Mag. Cloud Fraction	100%	64%	26%	11%	17%	15%	33%	25%

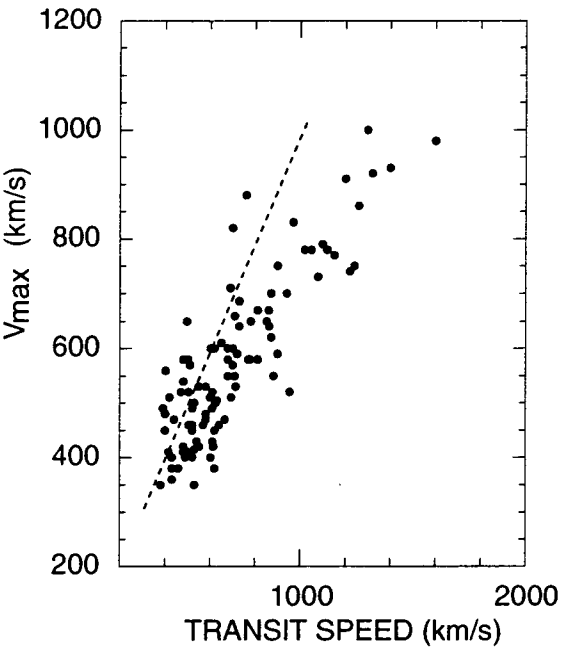
1200
1000
800
600
400
200
Vmax (km/s)
1000
2000
TRANSIT SPEED (km/s)

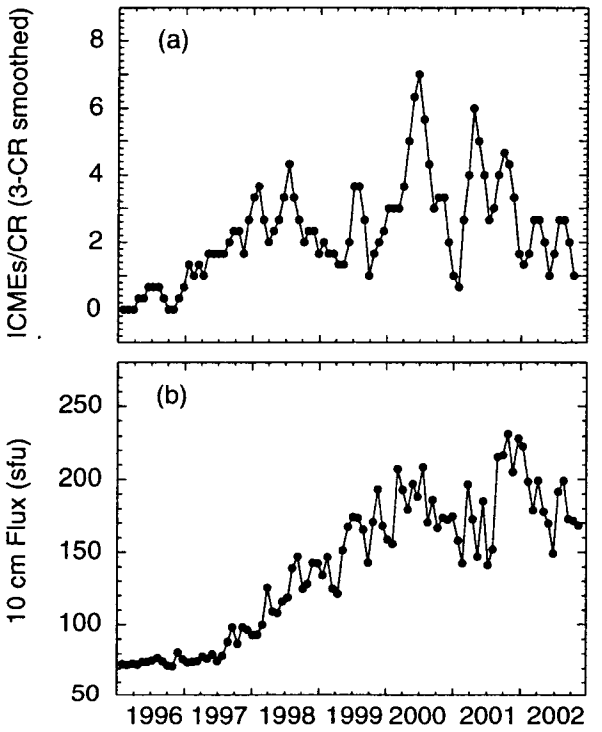
ICMEs/CR (3-CR smoothed)
(a)
8
6
4
2
0
10 cm Flux (sfu)
(b)
250
200
150
100
50
1996 1997 1998 1999 2000 2001 2002

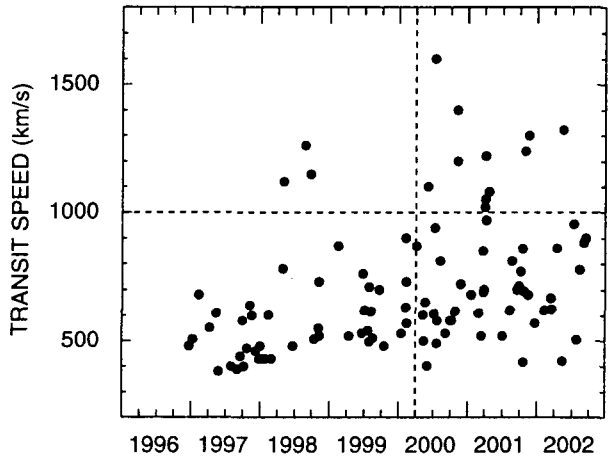
TRANSIT SPEED (km/s)
1500
1000
500
1996
1997
1998
1999
2000
2001
2002

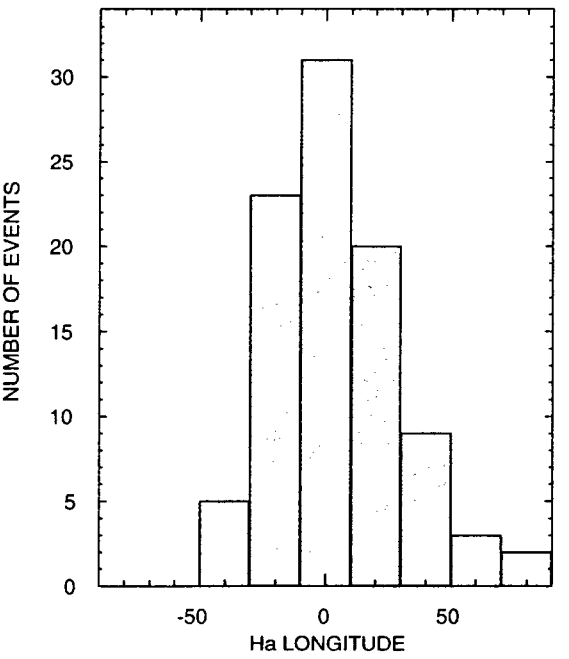
NUMBER OF EVENTS
30
25
20
15
10
5
0
-50
0
50
Ha LONGITUDE

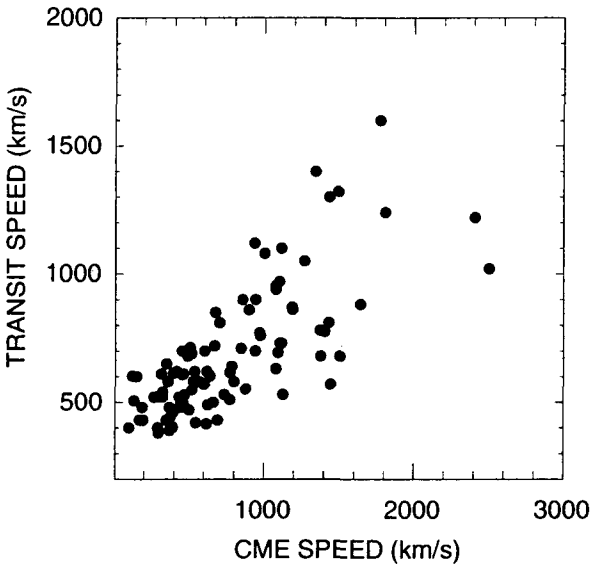
2000
1500
1000
500
TRANSIT SPEED (km/s)
1000
2000
3000
CME SPEED (km/s)

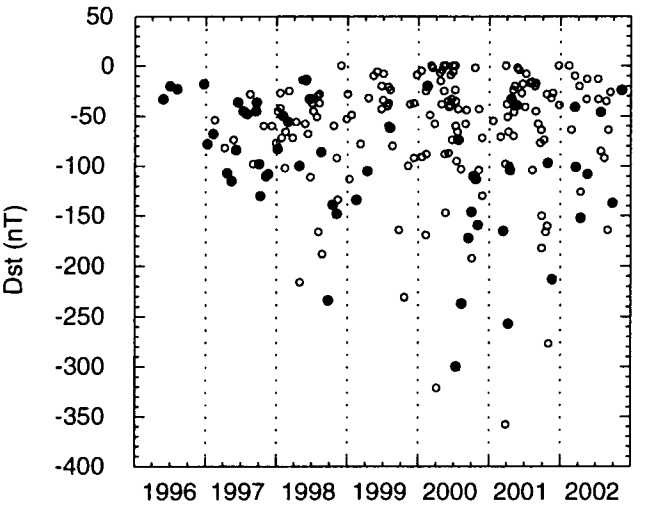
50
0
-50
-100
-150
-200
-250
-300
-350
-400
Dst (nT)
1996
1997
1998
1999
2000
2001
2002